Draft version 0.1

ATLAS NOTE

July 15, 2015

TGC Background Hit Rate: Comparison Between 2012 Data and Simulation

Y. Chan[a], T. Koi[b], I. Ravinovich[c], C. Young[b]

[a]*The Chinese University of Hong Kong, Shatin, Hong Kong*
[b]*SLAC National Accelerator Laboratory, Stanford, CA, USA*
[c]*Weizmann Institute of Science, Rehovot, Israel*

Abstract

This note compares the hit rates in TGC during Run 1 with simulation.

1 Introduction

Hit rates in the ATLAS Muon Spectrometer (MS) are dominated by background. Thus, understanding the background is important for both current operations and future upgrades. While simulated background has been compared with other detector measurements before, this is the first with Thin Gap Chambers (TGC). It is particularly relevant since similar chambers will be deployed in the New Small Wheel [1] upgrade.

The rest of this report is organized as follows. Section 2 is a brief description of the MS; Section 3 describes the background simlation tool; Section 4 details the analysis; and Section 5 is the comparison between simulation and data. Section 6 is the summary.

2 Muon Spectrometer: Thin Gap Chambers

Thin Gap Chambers are located in the endcap inner (EI) and endcap middle (EM) stations of the Muon Spectrometer. Figure 1 is a z-y quadrant view of the ATLAS detector. TGC chambers are in magenta.

The EI station is located behind the endcap calorimeter and in front of the endcap toroid, and has the highest hit rate in the entire MS. There are two main sources of background. One is from the front. Shower leakage from the calorimeter can penetrate the relatively thin disk shield on the front of the EI package. Secondary particles from p-p collisions hitting the unshielded beampipe section near $z = 7\,\mathrm{m}$ give rise to background which has a similar pathway through the disk shield. The second source is leakage from beamline shielding. This leakage can come through the bulk of the shielding material located radially between EI chambers and the beampipe, or it can migrate along the cracks between sections of shielding material. Care has been taken to minimize the size of cracks and to have chicanes instead of straight paths; however, such cracks are unavoidable in order to construct and assemble the detector.

The EM station is located behind the endcap toroid. Its primary source of background is leakage from beamline shielding, which can again be separated into bulk penetration and migration through cracks.

Improvements were made to the shielding during Long Shutdown 1 (LS1): better shielding at $z = 7\,\mathrm{m}$ and reducing the size of cracks between shields. [2] Other LS1 changes such as a new beampipe [3] are also expected to impact MS background. However, these modificationss have no impact on this study because the data involved in this report are from Run 1. And the simulation has the corresponding Run 1 geometry.

3 Simulation

We use the FLUGG-based [4] stand-alone cavern background application [5] for this work. Geometry is defined using Geant4 [6]. The sensitive detector elements, whose internal details are crucial for physics analysis but are unimportant here, have been simplified appropriately to improve computational performance. On the other hand, shielding and other beamline elements are more detailed since they are critical to background. Physics modeling is performed with FLUKA [7], which is the de-facto standard for shielding and background studies.

Particles produced in p-p collision events at $\sqrt{s} = 8\,\mathrm{TeV}$ generated using Phojet [8] as well as their decay and interaction daughter particles are tracked by the FLUGG application. Information recorded when they cross into any of the logical scoring volumes defined around each muon station includes particle type, 4-momentum, position and time. This incident flux is convoluted with path-length corrected, energy-dependent and technology specific sensitivities to obtain hit rates. For this study, we use the TGC sensitivities from the Radiation Background Task Force report [9]. Figure 2 and Figure 3 are the neutron

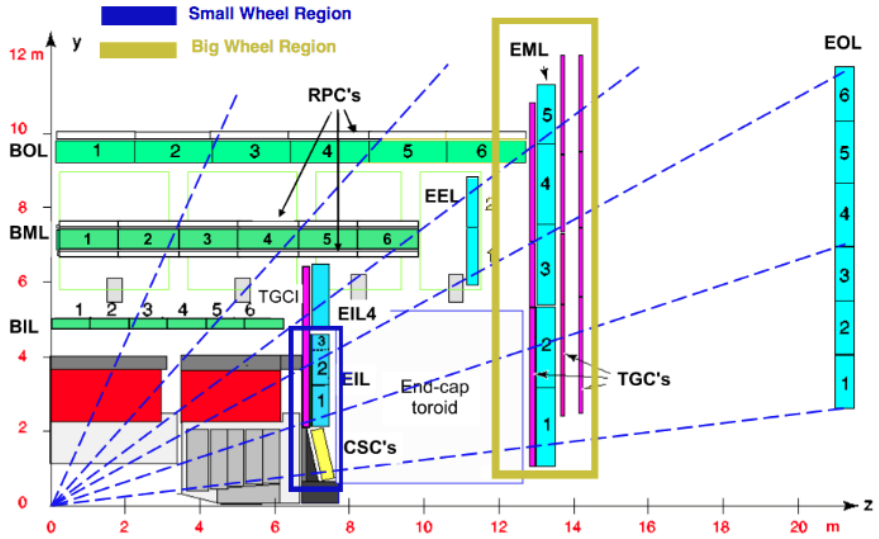

Figure 1: A z-y view of 1/4 of the ATLAS detector. This is a cut-out on the muon spectrometer at the large sectors, hence the names "Endcap Inner Large" (EIL), "Endcap Middle Large" (EML), etc. The Tin Gap Chambers, indicated by the magenta boxes, are used for triggering in the endcap region.

and photon sensitivities respectively. The red lines are the actual sensitivities used in this study, while the black points are the result of a closure test when applying the sensitivities.

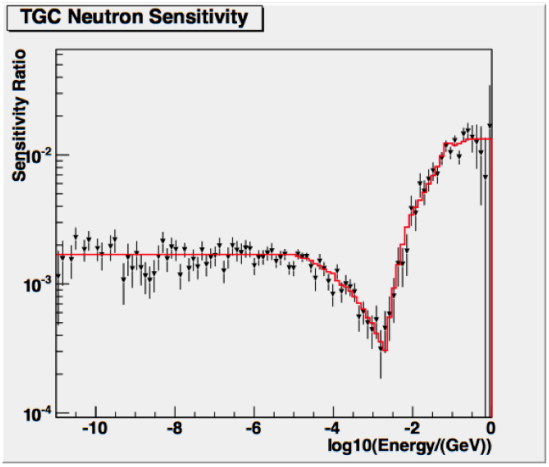

Figure 2: Single-plane sensitivity of TGC chambers to neutrons at normal incidence as a function of $\log_{10}$ of neutron kinetic energy in GeV. The red line is the actual sensitivity function used in this study, and black points are the result of a sample test.

The simulated hits are then normalized to get the number of hits per p-p events per unit area. It is often convenient to consider hit rates at a given luminosity. A cross section of $\sigma(pp) = 70\,\text{mb}$ [10] is used in the conversion.

The same application can produce radiation maps in a (z,r) grid using FLUKA's built-in functionality to accumulate user specified quantities. Total ionizing dose and 1-MeV neutron equivalent fluence aer

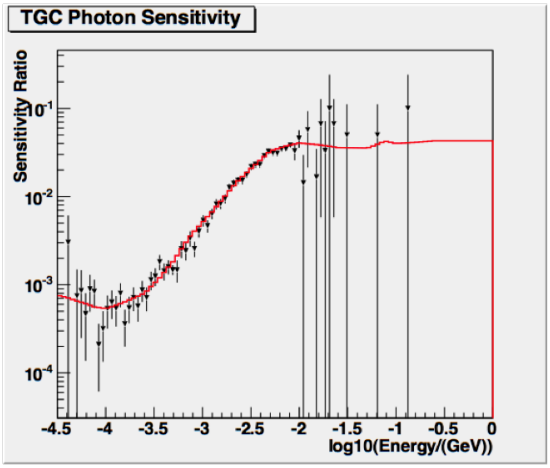

Figure 3: Single-plane sensitivity of TGC chambers to photons at normal incidence as a function of $\log_{10}$ of neutron kinetic energy in GeV. The red line is the actual sensitivity function used in this study, and black points are the result of a sample test.

among the available maps.

The predictions of the FLUGG application have bee validated by comparing with Run 1 measurements. The radiation Estimation Task Force examined:

- RPC HV current [11]
- MDT hit rates
- RADMON measurements of dose and fluence [12]
- dosimeter measurements [13]
- MPX hit rates [14]

and concluded that there was a generally good level of agreement. [15]

4 TGC Run-1 2012 data analysis

In this section we shortly describe the analysis of the TGC data in the present SW and BW of the ATLAS Experiment. The data set used for this analysis:

- Run-1, November 15th, 2012, run number 214553. The peak luminosity during this run was 6.69x10^{33} Hz/cm^2, the average luminosity was 3.80x10^{33} Hz/cm^2.
- Trigger: the trigger which has been used for this analysis was L1_RD0_FILLED. The number of the recorded/analyzed events with the above trigger is 720474 events.
- The detectors used in this analysis are TGC (T10) doublets from SW FI, 24 detectors from each side (A and C) and TGC (T1, T3, T6, T7 and T8) triplets from BW M1, FW and EC, 48 detectors from each side as well.

The bunch crossing distributions are shown in Figure 4. The length of each bunch crossing (previous, current and next) is 25 ns. Only central bunches have been used in the present analysis.

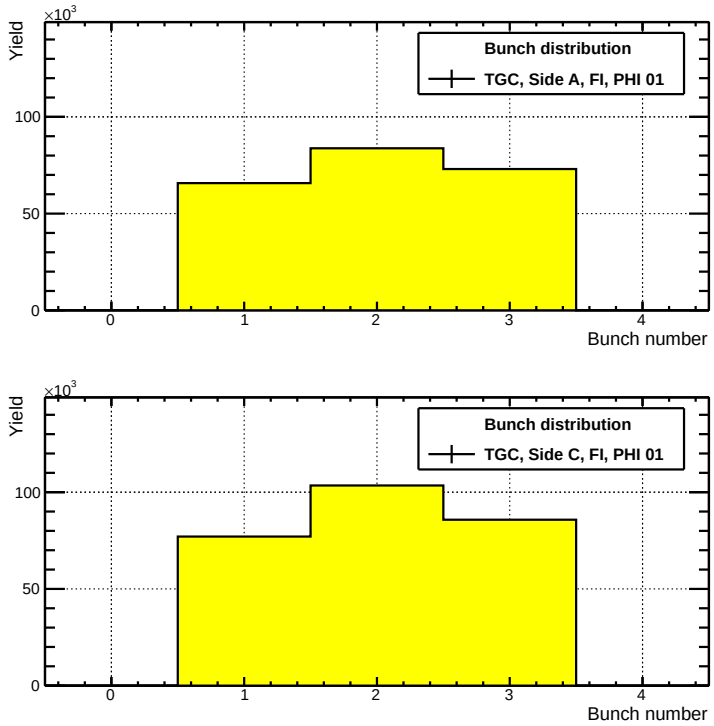

Figure 4: Bunch crossing distribution for a trigger L1_RD0_FILLED.

The first step of the analysis was to extract the number of hits per event in the first gas gap, namely Layer-1. What we call a hit is a fired wire together with a strip partner. The extracted number of hits versus wire group position has been then normalized to the area of each group of ganged wires and to the length of a single bunch, namely 25 ns. These extracted hit rates as a function of the radius are shown in Figure 5 (for SW) and in Figure 6 (for BW), separately for side A (top plots) and side C (bottom plots). In order to increase the statistics and consequently reduce the error bars all working detectors on each side A and C were combined together. Before going this way the have verified that there is no ϕ dependence.

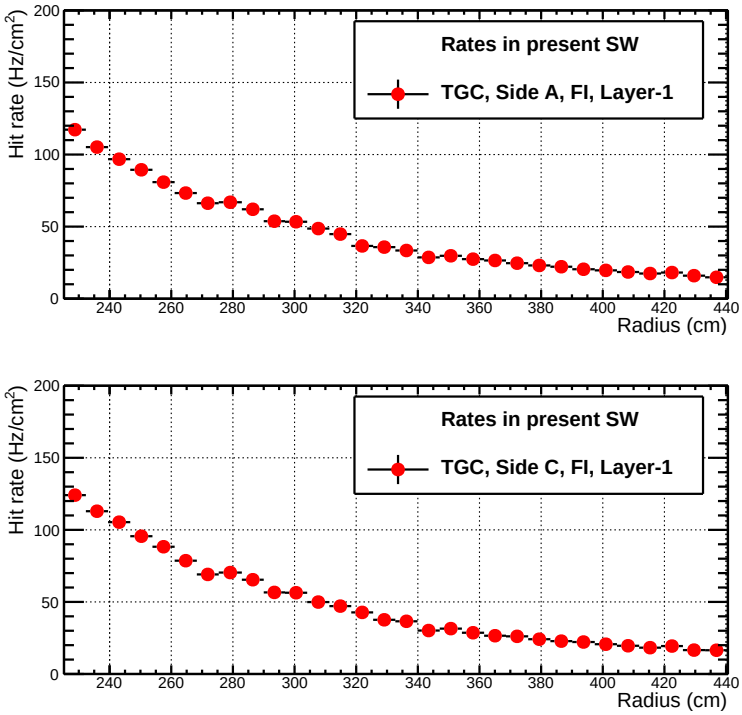

Figure 5: Hit rate distribution in SW as a function of a radius.

The next goal for the present analysis was to extract the average charge per hit. For that we used the TGC HV current information recorded during this run by DCS. The current distributions are shown in Figure 7 for side A (top plot) and side C (bottom plot) separately. Using the average current and the average hit rate from each side the average charge per hit has been calculated:

- Side A: $< Q > = 3.81 \pm 0.07$ pC
- Side C: $< Q > = 4.47 \pm 0.09$ pC

The errors for the average charge above reflect only the statistical accuracy of the average HV currents recorded by DCS. The statistical error of the hit rate determination is negligible. The systematic uncertainty will be studied later.

The last step of this analysis was to extract the correlated rates. For this both gas gaps, namely Layer-1 and Layer-2, from TGC doublets have been used. The definition of the hit in this case is a coincidence between two hits from each gas gap. The nice correlated peaks are seen in both sides as it is shown Figure 8 (left, top and bottom rows). The extracted correlated rates are also shown in Figure 8 (right, top and bottom rows).

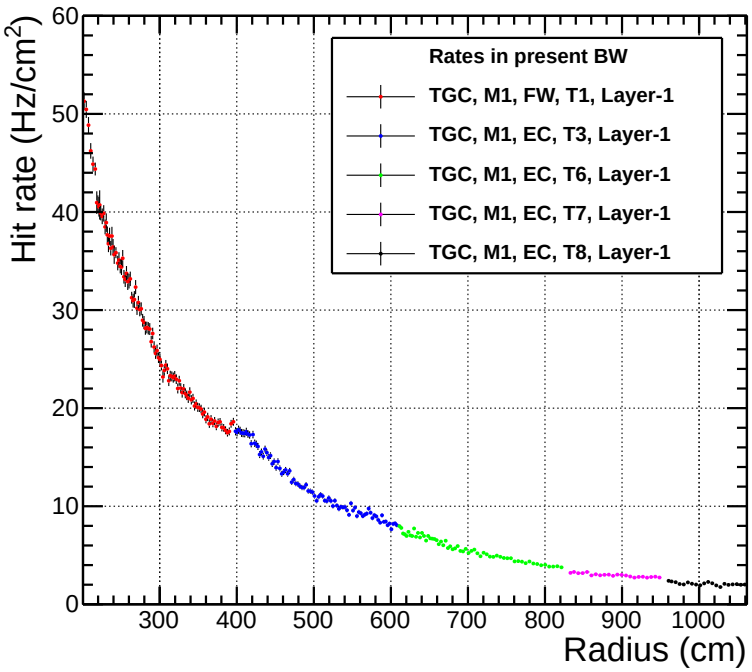

Figure 6: Hit rate distribution in BW as a function of a radius.

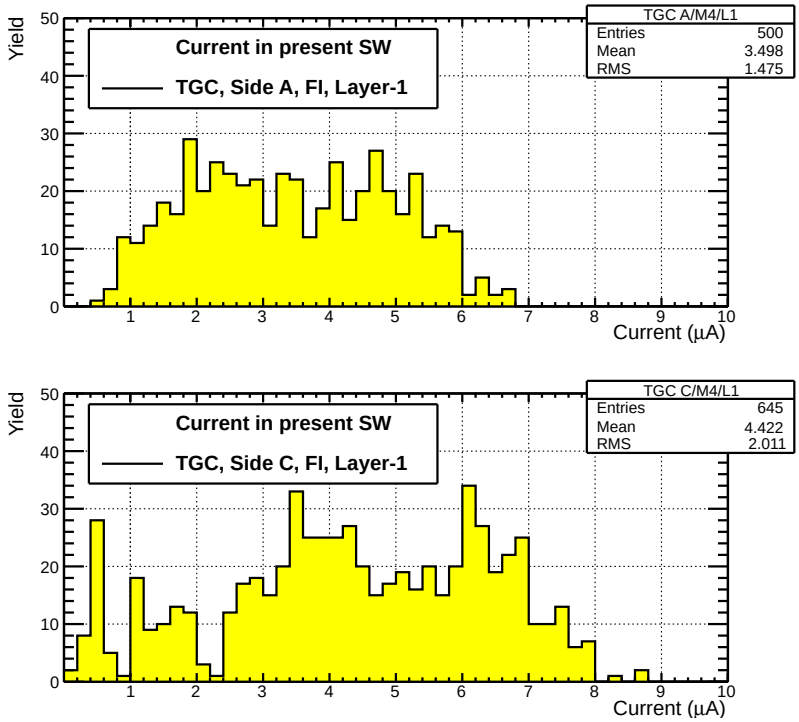

Figure 7: TGC current distribution recorded by DCS

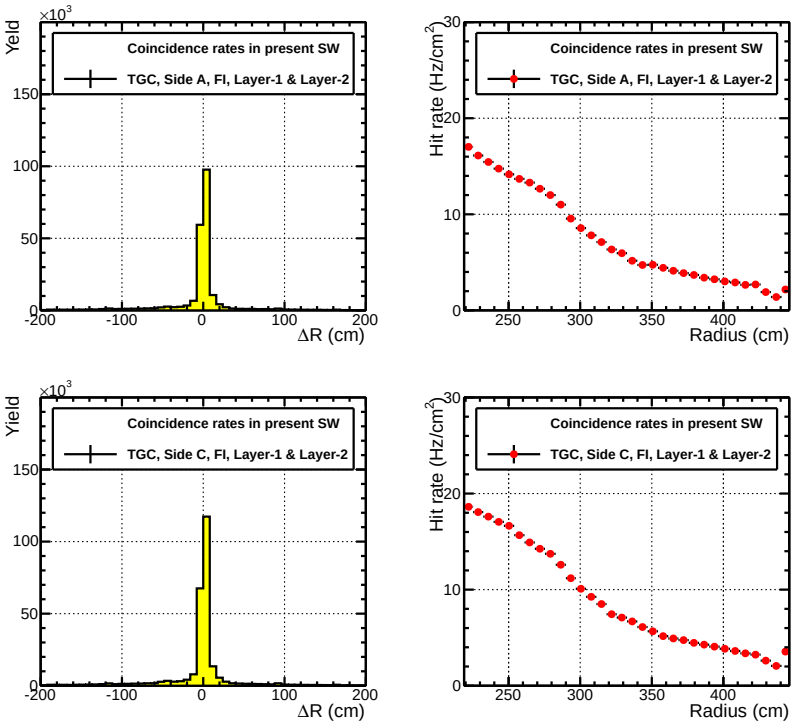

Figure 8: Matching distribution of correlated hits in two layers (left plots) and correlated rates (right plots).

5 Comparison with Simulation

The background simulation application described in Section 3 has been used to predict the MS hit rates for detector geometries and beam energies relevant for Run 1 and Run 2 [18]. The simulation have been rebinned to provide a direct comparison with the measurements here. The comparison between the TGC hits from Run-1 2012 data, described in Section 4, has been performed for both SW and BW. These comparisons are shown in Figure 9 (for SW) and in Figure 10 (for BW).

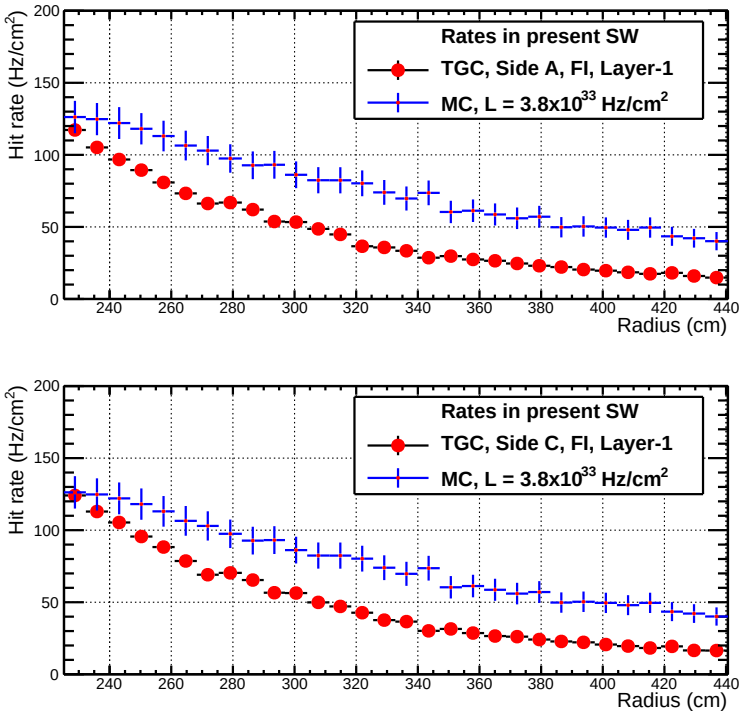

Figure 9: Comparison of the hit rates measured in TGC SW with MC simulations.

One can see from these figures that the MC predictions are systematically higher than the data, both in SW and BW measured ranges.

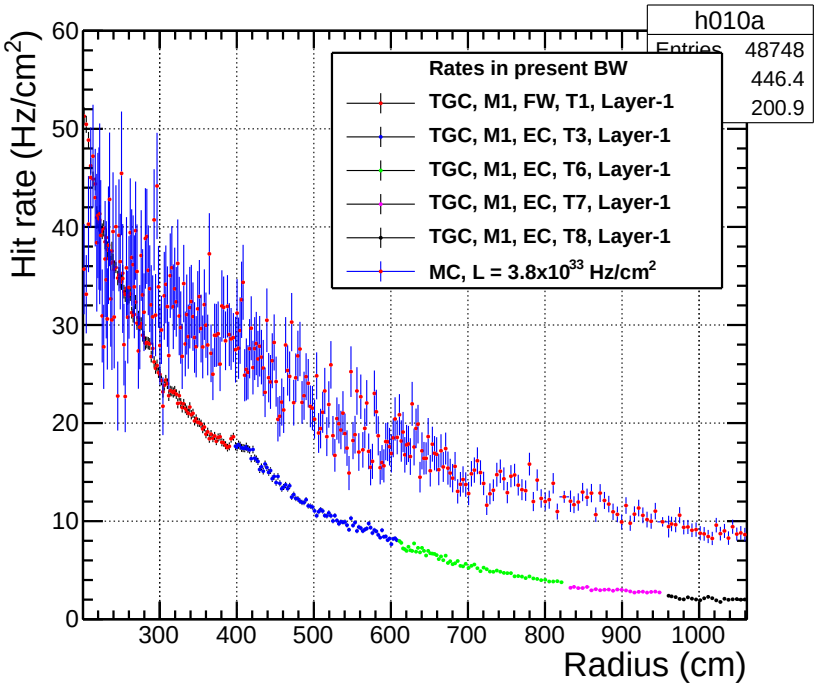

Figure 10: Comparison of the hit rates measured in TGC BW with MC simulations.

References

[1] New Small Wheel Technical Design Report, ATLAS-TDR-020.

[2] Additional LAr-JD Shielding, Giancarlo Spigo, ATL-MH-ER-0024.

[3] reference to new beam pipe deaign.

[4] FLUGG, http://www.fluka.org/content/tools/flugg/index.html

[5] ATLAS internal note describing FLUGG based application for cavern background calculation, ATL-COM-SOFT-2011-032.

[6] Geant4 Toolkit, Nuclear Instruments and Methods in Physics Research A 506 (2003) 250-303; IEEE Transactions on Nuclear Science 53 No. 1 (2006) 270-278

[7] "The FLUKA code: Description and benchmarking", G. Battistoni, S. Muraro, P.R. Sala, F. Cerutti, A. Ferrari, S. Roesler, A. Fasso', J. Ranft, Proceedings of the Hadronic Shower Simulation Workshop 2006, Fermilab 6–8 September 2006, M. Albrow, R. Raja eds., AIP Conference Proceeding 896, 31-49, (2007); "FLUKA: a multi-particle transport code", A. Fasso', A. Ferrari, J. Ranft, and P.R. Sala, CERN-2005-10 (2005), INFN/TC-05/11, SLAC-R-773

[8] R. Engel, PHOJET Manual, http://physik.uni-leipzig.de/~eng/phojet.html

[9] Radiation Background Task Force Report, ATL-GEN-2005-001.

[10] ATLAS has measured an inelastic cross section of 69.4 ± 2.3 (exp) ± 6.9 (extrap) mb at $\sqrt{s} = 7$ TeV, Nature Commun. 2 (2011) 463.

[11] G. Aielli, Cavern background measurement with the ATLAS RPC system. https://cds.cern.ch/record/1457509

[12] ATL-COM-GEN-2013-004, https://cds.cern.ch/record/1544075?ln=en

[13] See talk by C. Young, https://indico.cern.ch/conferenceDisplay.py?confId=249160

[14] ATL-COM-GEN-2013-003, https://cds.cern.ch/record/1543444?

[15] See talk by F. Lanni during ATLAS Upgrade Week (May 2013), https://indico.cern.ch/event/233533/session/32/contribution/188/material/slides/0.pdf; report to be available as EDMS ID 1293497 https://edms.cern.ch/document/1293497/1

[16] Shielding Project web page, http://atlas.web.cern.ch/Atlas/GROUPS/Shielding/shielding.htm

[17] Polyethylene with 5% boron in the form of B_4C. The high hydrogen content thermalizes fast neutrons and the boron attenuates thermal neutrons through capture.

[18] Expected Muon Spectrometer Background in Run 2, ATL-COM-MUON-2014-027.